WU Liangjun, WANG Pujun, ZHANG Jing, et al. Sedimentary and palaeoclimatic characteristics of planation surface at the edge of typical karst plateau: A case study of Luota and Jiaba sctions in Xiangxi[J]. Carsologica Sinica, 2024, 43(2): 253-271.
DOI: 10.11932/karst20240202

Sedimentary and palaeoclimatic characteristics of planation surface at the edge of typical karst plateau: A case study of Luota and Jiaba sctions in Xiangxi

WU Liangjun[1,2,3], WANG Pujun[1], ZHANG Jing[2,3], XIN Cunlin[4], RONG Yuebing[2,3], CHEN Weihai[2,3], ZHANG Yuanhai[2,3], HUANG Chao[5]

(1. *College of Earth Sciences*, *Jilin University*, *Changchun*, *Jilin* 130061, *China*; 2. *Institute of Karst Geology*, *CAGS/Key Laboratory of Karst Dynamics*, *MNR & GZAR/International Research Center on Karst under the Auspices of UNESCO*, *Guilin*, *Guangxi* 541004, *China*; 3. *Pingguo Guangxi*, *Karst Ecosystem*, *National Observation and Research Station*, *Pingguo*, *Guangxi* 531406, *China*; 4. *College of Geography and Environmental Science*, *Northwest Normal University*, *Lanzhou*, *Gansu* 730070, *China*; 5. *Survey and Monitoring Institute of Hydrogeology and Environmental Geology of Hunan Province*, *Changsha*, *Hunan* 410003, *China*)

Abstract The palaeoenvironment has an important influence on the formation and evolution of karst geomorphology, and the planation surface at the edge of the karst plateau is one of the important recorders. The Yunnan−Guizhou Plateau is an important karst plateau in China, on the southeast edge of which is located Xiangxi in Hunan Province—a deep cut platform and gorge development area. Xiangxi is also a combination zone of low mountains and middle mountains at the edge of the Yunnan−Guizhou Plateau, in which the high plain transits to the alluvial plain, with rich records of planation surfaces. These planation surfaces are characterized by rapid altitude changes, different weathering crust materials and different types of bedrock lithology. However, the weathering crust properties and palaeoclimate characteristics of these planation surfaces are still unclear. Therefore, we choose two weathering crusts representing the elevation of 1,400 m and 600−700 m of planation surfaces in Luota Period (Luota section) and Zhaoshi Period (Jiaba section) as study objects. In this study, conducting the inversion of palaeoclimate indicated by weathering crusts of planation surfaces through grain size, magnetic susceptibility and sporopollen analyses, we hope to provide more evidence for the development characteristics of planation surfaces and palaeoclimate evolution on the edge of the Yunnan−Guizhou Plateau.

Results show that the weathering crust of Luota section is 5.0 m thick and can be divided into 5 layers. The lithology is mainly composed of humus, gravel layer, silt, clay, etc. The content of silt with sizes ranging from 5 to 50 μm is the highest, accounting for 57.6%; the average content of clay is 41.9%; the sand content is the lowest, at 0.56%, all of which are fine sand. The weathering crust in Jiaba section is 3.5 m thick and can be divided into two layers. The lithology is mainly composed of humus, silty, clay and a small amount of gravel. The content of silt with sizes ranging from 5 to 50 μm is also the highest, accounting for 54%; the average content of clay is 39%. In addition, the analyses of Md, Mz, σ, Sk, Kg, SC/D values, magnetic susceptibility and other indicators show that there appear multiple index fluctuations in both Luota and Jiaba sections, but the fluctuation range of Jiaba section is relatively limited. The types of sporopollen in the two sections are different. Luota section is mainly composed of *Polypodium* and *Pinus*, with a small number of *Abies*, *Podcarpus* and *Chenopodium*. The main sporopollen components of Jiaba section are *Polypodium* and *Pinus*, and a few *Gramineae* and *Carpinipites* are found. The types of sporopollen in Jiaba section are fewer than those in Luota section, and the concentrations are also lower. Based on the development of *Polypodium* in both sections, it is supposed that the climate during the sedimentary period of weathering crust was warm and hot. However, the climate during the sedimentary period of Luota section may have been a warm climate with high

humidity, while the climate of Jiaba section may have been a cool and humid climate with low humidity. In addition, according to the analysis of sporopollen and the previous data, it is speculated that the weathering crust of Luota section may have been formed in the early Neogene, and the planation surface may have been formed in the Miocene. The weathering crust of Jiaba section may have been formed in the early Quaternary, and the planation surface may have been formed in the Pleistocene.

Key words Xiangxi UNESCO Global Geopark, planation surface, palaeoclimate, grain size, magnetic susceptibility, sporopollen

0 Introduction

The Yunnan−Guizhou Plateau (YGP) is a typical karst plateau in China. After multiple uneven uplifts caused by the Himalayan tectonic movement, combined with water erosion and other effects, ancient planation surfaces with various cutting forms have been widely formed at the edge of YGP. This kind of landform is characterized by a close interaction between the plateau and canyon landforms and is very different from the clastic rock plateau. The combination of platform and canyons on the edge of karst plateau can form a dense network, which is more sensitive to the rate of plateau uplift and the intensity of tectonic movement. It also records richer evolutionary information for the karst biological environment system based on karst landforms. Distributed in various latitudes of the Earth[1], ancient planation surfaces play an extremely important role in the formation and evolution of mountains and in the differentiation of regional landforms[2]. Therefore, ancient planation surfaces have been applied to multiple geological research fields such as structure, sedimentation, and geomorphological evolution. For example, planation surfaces were used in the studies on uplift amplitude of the Qinghai−Tibet Plateau[3-5], besides the studies on stages, forms[6-7] and characteristics[8] of neotectonic movements. The accompanying weathering crust and cover layer can be used to constrain the ancient climate[9-11], and can also establish connections between the geomorphic evolution of different plateaus, such as the Qinghai−Tibet Plateau and the YGP[3, 8, 12-14].

Xiangxi is located in a low-middle mountain junction zone at the edge of the YGP that transits from high plain to alluvial plain[15] (Fig.1). Xiangxi UNESCO Global Geopark, in which a magnificent landform of terrace canyon group has been developed [16-17], is listed as an important component of world-class geoheritage by UNESCO[18]. The erosion and planation of the terrace canyon group in Xiangxi is very prominent. According to previous research data, there may be three periods of large-scale tectonic uplift and stable cycles in the Hunan−Guizhou−Hubei region. The first period experienced the crustal uplift at the end of the Cretaceous and the uplift gradually stabilized in the Cenozoic. In this period, the first-level planation surface—the Dalushan Period—was formed, with an elevation of about 1,600−2,000 meters. The planation surface of this period was eroded for a long time and remained little in the study area. Subsequently, in the Miocene, the Xiangxi region continued to rise and stabilize, forming the second-level planation surface with an altitude of 1,000−1,400 meters. This planation surface belongs to the Luota period, also known as the Shanpen period, in which the terrace was more developed. Since the Pleistocene, the Xiangxi region once again rose, with rivers strongly cutting downwards, forming the third-level planation surface with an altitude of about 600−700 m. This planation surface belongs to the Zhaoshi period or the Wujiang period, and is mainly characterized by valley landforms. In the Xiangxi region, effects of planation surface in the Luota period and the Zhaoshi period are more developed, representing a dynamic response of significant differences in the intensity of tectonic movement within the region[19]. The products of these two main periods can be divided into approximately 6 levels of planation surfaces (Table 1) [19-21], and various unexposed karst micro-landforms have been formed[6].

For planation surfaces in these two periods in Xi-

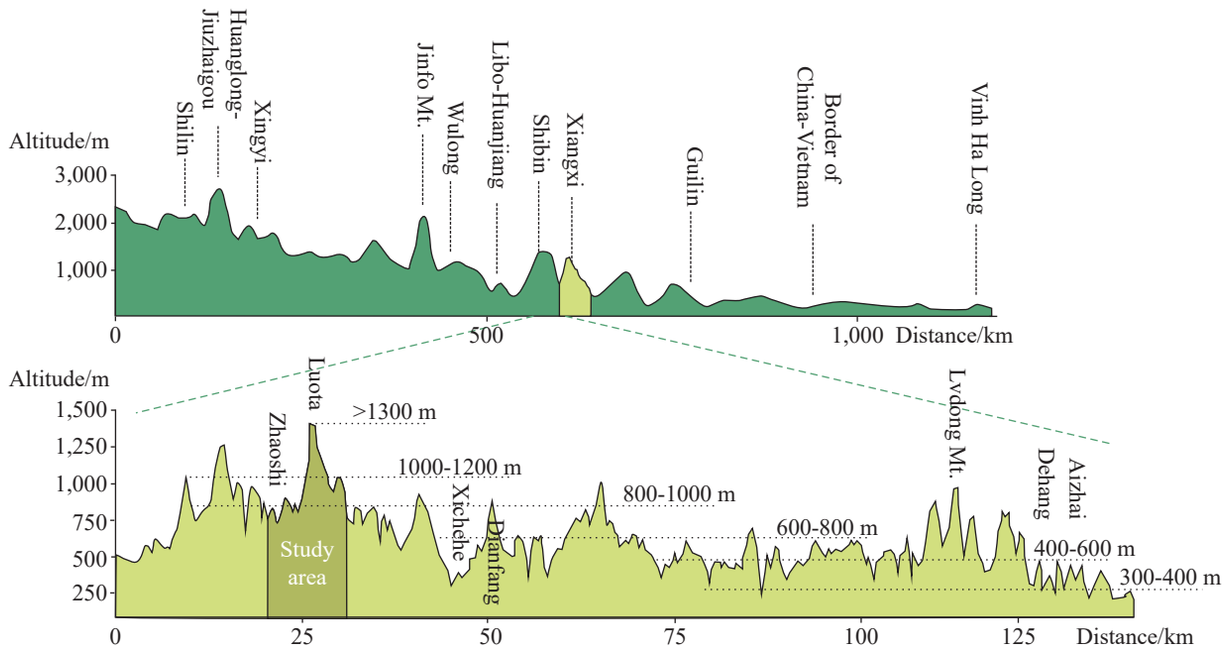

Fig. 1 Elevation profile of the karst area in Southwest China and distribution of the planation surface in Xiangxi

angxi, CHEN[19] studied their development characteristics and classification, and believed that there is a north-south imbalance in planation surfaces in the region, and the weathering crust above the planation surface may record the intensity of uplift and environmental changes. YU et al[22] studied bedrock characteristics of planation surface and believed the bedrock is the controlling factor of karst micro-landforms above the planation surface. Moreover, they divided karst micro-landforms into 9 types and emphasized the influence of environmental conditions, such as paleohydrology, on landforms. JIN et al[20] discussed the development history of the Luota platform and divided its development into 5 stages. During the development, the extensive accumulation of clay deposits closely related to environmental changes may have occurred during the Early to Middle Pleistocene. PENG et al[10] studied the Quaternary deposits in Luota and its surrounding areas, and found that there are different compositions in deposits at different altitudes. The deposits on the Luota platform are endogenous deposits, and there may be multiple sources around the platform. Studies on elemental characteristics of deposits found that there may have been a warm and humid climate in this region during the early to middle Pleistocene. LAO et al[11] analyzed the characteristics of the karst surface zone and pointed out that climate is an extremely important external condition for karst development. YIN[23] and ZHANG et al[24] found that there were climate fluctuations in the middle and late Holocene, which were related to the atmospheric circulation and solar radiation background at the hemispherical scale. Based on their climatic research of the stalagmites of Lianhua cave in the Luota area, there may have occurred multiple changes during the Quaternary. Many scholars have conducted research on the structure[25-28] and hydrology[29-32] of the Xiangxi region, but currently, the weathering crust properties and paleoclimate characteristics of planation surface in these two periods are not clear. Although planation surfaces in these two periods are close to each other (Fig.2), there is a significant elevation difference, and they are located in different bedrock areas (carbonate and clastic rocks), with different material sources. Therefore, the study of the planation surfaces in these two periods will help to compare lithology differences at different elevations and bedrock, and to conduct inversion of paleoclimate when the planation surfaces were formed, providing more evidence for the development characteristics of planation surfaces at the edge of the

Table 1 Development characteristics of karst landform and planation surface in Xiangxi

No.	Karst stratification	Level of planation surface (north)[19]	Example of planation surface (mountain)[19]	Period of platform [20-21]	Elevation of platform (m)	Deposit [21]	Forming age of platform (Speculation)[19-21]	Combination of landform
1		Level 1-2		Tiziyan period	> 1,300	Residual slope, ice water accumulation	Paleogene	Solitary peaks, ponors, residual caves, stone forests, karst hills
2	Layer I	Level 3	Huping mountaom, Xihai, Xihuang mountain, Laer mountain, Daqingshan, etc.	Badongxiansha n period	1,230	Red gravel accumulation	Neogene	karst hills, dolines, karst depressions, shafts, karst ridges, clints, stone forests, ponors
3				Yabusi period	1,030	Flowing water phase accumulation	Late Neogene−Early Quaternary	karst hills, deep valleys, karst ridges, stone forests, clints
4	Layer II	Level 4	Damijie, Hejia mountain, Paibi, etc.	Luota valley period(High valley−wide valley−Cheshu iping river sub-stage)	650−900	Red-yellow clay sand gravel, gray black silt	Pleistocene	valleys, canyons, karst hills
5	Layer III	Level 5	Baofeng lake, Nanhua mountain, etc.	Luota valley period(canyon sub-stage)	400−600	Sand gravel, sub-clay	Holocene	Underground rivers, horizontal karst caves, dolines, karst depressions
6	Layer IV	Level 6	Both sides of the Yuanshui river and Lishui river	Modern period	300−400	Clay, gravel	Holocene	horizontal karst caves, shallow karst depressions, shallow dolines, swallet streams

YGP as well as for the evolution of paleoclimate.

1 Overview of the study area

The study area is located in the northwest of Hunan Province. Geographically, it is in the southern section of the turning part between the second and third geomorphologic steps of China. Geologically, it is located in the transitional zone on the southeastern edge of the Yangtze Block and the eastern edge of the Yunnan−Guizhou Uplift, adjacent to the South China block. Since the Yanshan movement, a giant Neocathaysian tectonic system has been formed in the area and has undergone multiple periods of tectonic influence. This has led to the crisscrossing of faults in the surrounding areas, characterized by the formation of synclines into mountains and anticlines into valleys (Fig.2). The strata are composed of Cambrian, Ordovician, Silurian, Permian, Triassic, and Quaternary strata, with a thickness of 880−1,160 m. After the Paleogene, the folds and mountains formed in the early stages were gradually eroded due to erosion and changes in the baseline, ultimately forming comparable two-level large-scale planation surfaces in Xiangxi. These surfaces are the Luota planation surface (1,400 m) and the Zhaoshi planation surface (600−700 m) (Fig.3). Although different scholars may differently name the planation surfaces in these two periods based on the landmark landforms of different regions[19], they actually refer to the same planation surfaces.

The planation surface in the Luota Period is one of the largest ancient planation surfaces in Xiangxi[19]. In the study area, this planation surface mainly presents it-

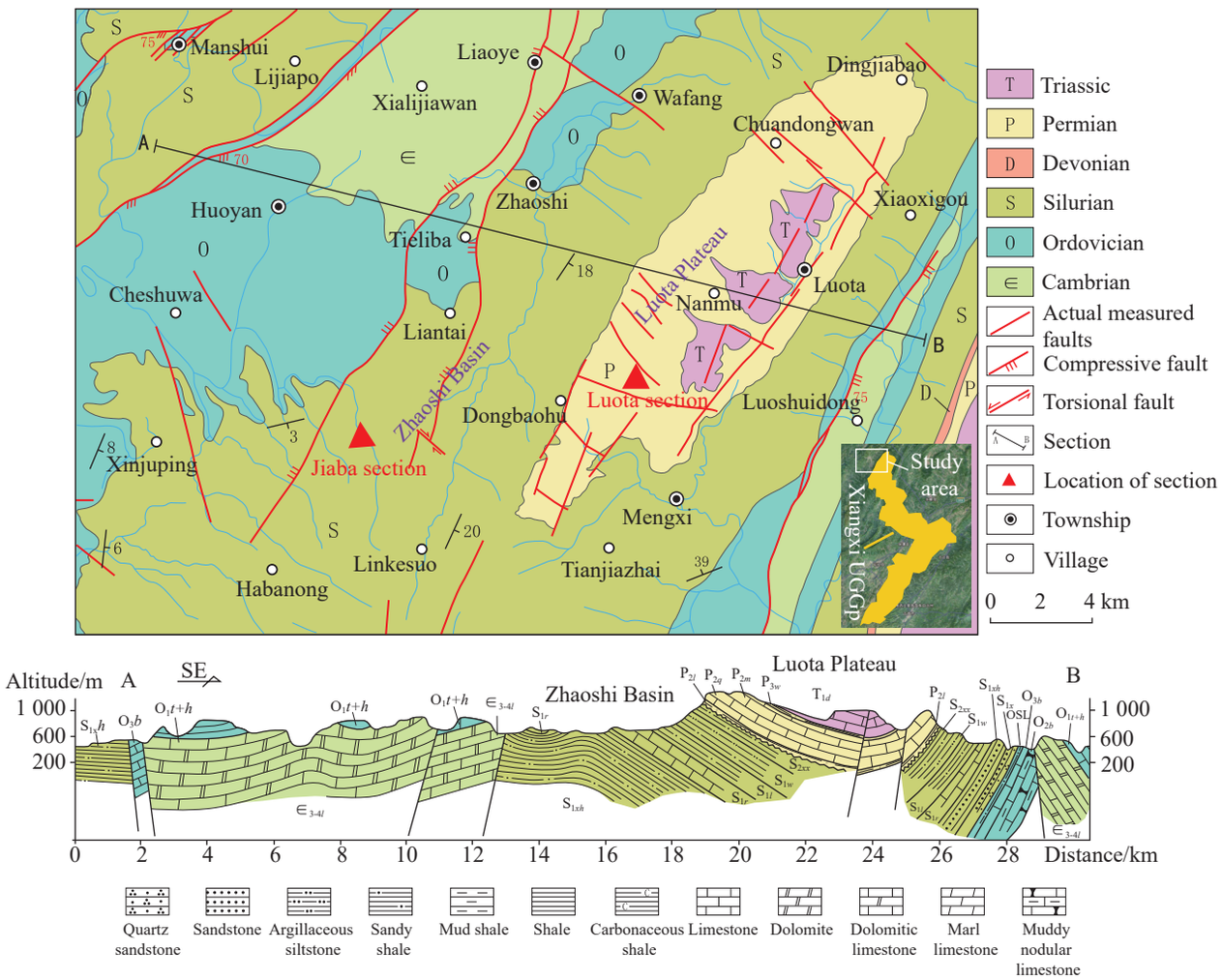

Fig. 2　Geology of Luota−Zhaoshi area in Xiangxi

Fig. 3　Realistic view of the planation surface in Luota period and Zhaoshi period

self as a northeast-oriented karst platform—the Luota platform, with an area of about 82 km^2 and a maximum elevation of 1,437 m. This geosite was formed by the erosion and cutting of the Luota river which inherited the original synclinal valley. At an altitude of 600−700 m, the planation surface in the Zhaoshi period is characterized by a northeast-oriented Zhaoshi basin located on the west side of the Luota platform. The main types of landforms of this planation surface are karst depressions, residual plateaus, karst hills, etc. The bedrock of the Luota platform is the Permian (Maokou Formation) mudstone and dolomite limestone, while the bedrock of the Zhaoshi basin is the Silurian (Xiaoheba Formation) fine sandstone, siltstone, and shale.

2 Research methods

2.1 Sampling

A detailed investigation was conducted on the geomorphology and stratigraphy of the planation surfaces in these two periods mentioned above. Luota section and Jiaba section were selected for measurement, representing the Luota and Zhaoshi planation surfaces, respectively. These two sections were recorded as 0 m on the soil surface, and the thickness of each sedimentary layer downwards was measured with a tape measure. To ensure the freshness of samples, 20-centimeter-thick topsoil from the layer was firstly removed, and cylindrical steel pipes were chiseled into the layer to collect samples. With an equidistance principle, 30 samples were collected from the 150−500-centimeter weathering crust of Luota section and 15 samples from the 50−350-centimeter weathering crust of Jiaba section. To avoid contamination from the upper layer to the lower layer, the sampling was completed from the bottom to the top. Synchronously, pollen samples were collected in the sections. The lithology of the weathering crust in Luota section is relatively rich, and hence 10 pollen samples were collected. Due to the relative lithological singularity of the weathering crust in Jiaba section, four pollen samples were collected. The sample numbers for the Luota and Jiaba sections were coded and started with abbreviations of Chinese Pinyin: LT- for Luota section, and JB- for Jiaba section.

2.1.1 Overview of Luota section

Luota section is located in a depression near Luota township, Longshan county. Due to the nearby village road renovation, this section left a fresh excavated surface (Fig.4), with a total thickness of about 5 meters. The covering layer is well exposed and clearly layered, which is conducive to systematic sampling. The geomorphic unit there belongs to the Luota platform.

2.1.2 Overview of Jiaba section

Jiaba section is located in Jiaba village, Zhaoshi town, Longshan county. Due to villagers' house building on a slope, this section left a fresh surface after excavation (Fig.5), with a total thickness of about 6.5 m. The geomorphic unit belongs to the Zhaoshi basin, close

	Lithology	Accumulated thickness/cm	Lithological description
5 m		40	Dark brown, red humus soil layer, vegetation.
		110	Brown loose deposits, mud and gravel layers, gradually increasing in gravel from top to bottom.
		110	Grey black, yellow brown, and brownish red clayey-silt and sandy-clay interbedded, forming the top of the weathered crust.
		30	Brownish yellow coarse sandstone interbedded with gravel.
		210	Brown gray clay and yellow brown clay interlayered, forming the bottom of the weathered crust.
	Road		

Fig. 4 Stratigraphic histogram of Luota section

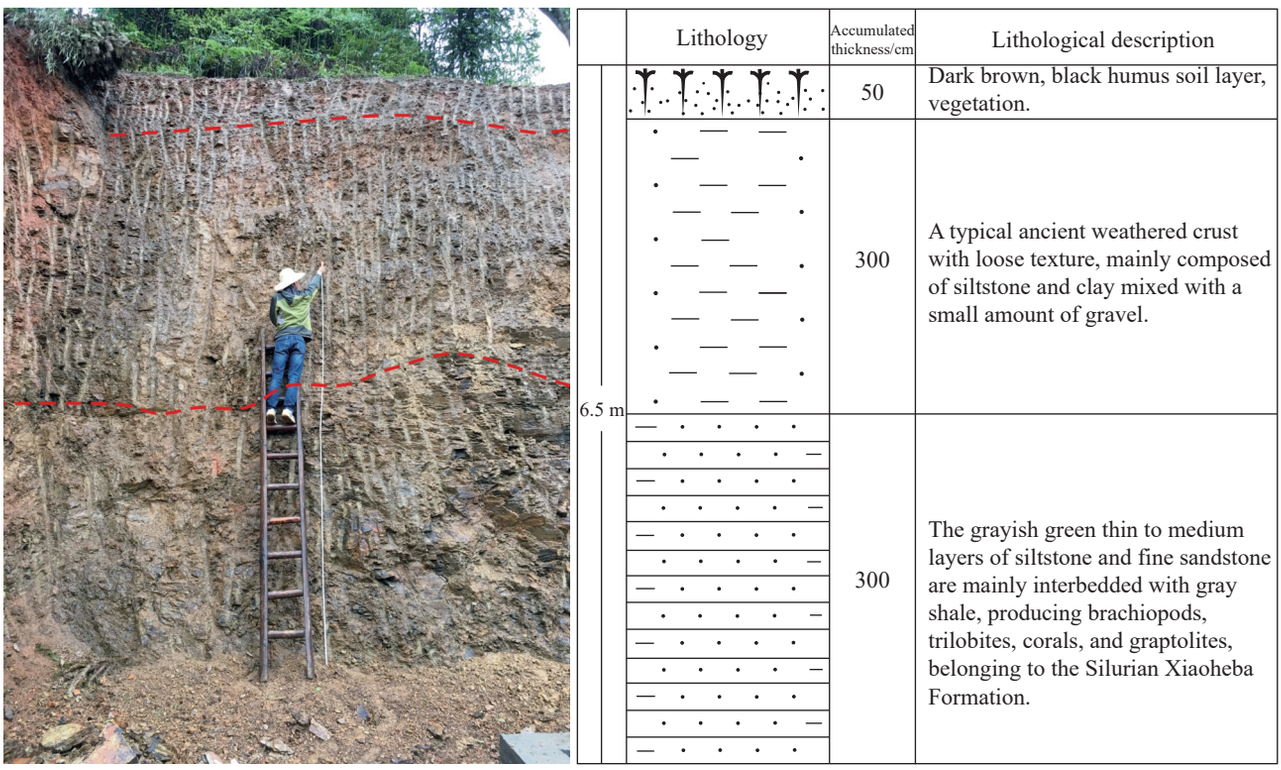

Fig. 5　Stratigraphic histogram of Jiaba section

to the Luota platform and near the geomorphic transition zone.

2.2　Analysis methods

In order to explore the paleoclimatic information recorded by the planation surfaces, field surveys and measurements on two sections were completed, and then a systematically analysis was conducted on lithological characteristics, composition of sediment particle size, characteristics of magnetic susceptibility, and composition of spore pollen.

2.2.1　Effects of particle size, magnetic susceptibility, and spore pollen

(1) Significance of particle size as a climate indicator

Particle size compositions of sediments usually vary in different environments; therefore, particle size characteristics can indirectly indicate sedimentary facies and climate changes[33-34]. For example, the particle size composition is used as an alternative indicator to reveal the effects of the East Asian winter and summer monsoons[35]. Sand particles can reflect desertification and climate change, indicating the strength of winter monsoon changes[36-37], while clay particles are closely related to weathering and soil formation, and can reflect the strength of summer monsoon changes[35-36]. Previous studies[37-42] believed that the higher the clay content is, the stronger it affects the soil formation and the stronger the summer monsoon becomes, and vice versa. At the same time, high values of mean grain size (Mz) and median diameter (Md) of sediment indicate that the climate is relatively warm and humid, and the degree of weathering is high. Conversely, low values indicate relatively cold and dry climate and weak weathering. In addition, the application of the particle size sensitivity values (SC/D, ratio of silt and clay to sand) can amplify the proportion relationship of particulate matter >4.32 Φ/<4.32 Φ, and the relationship can reflect the intensity of wind−sand activity. Under cold and dry conditions, winter wind is strong, and contents of silt and clay particles are relatively less than those of sand, with low SC/D. However, under warm and humid conditions, contents of silt and clay particles are relatively more than those of sand, with high SC/D.

(2) Significance of magnetic susceptibility as a climate indicator

The magnetic susceptibility (MS) is a physical quantity that reflects the degree of magnetization of a unit substance. MS of rock is controlled by factors such as type, content, and particle size of the magnetic minerals which the rock contains. MS of rock is the sum of the values of magnetic susceptibility of various magnetic minerals in the sample[43-44]. Magnetic minerals are divided into diamagnetic minerals, paramagnetic minerals, and ferromagnetic minerals. Common diamagnetic minerals include quartz, apatite, etc. Paramagnetic minerals include the majority of pure minerals such as dolomite, while ferromagnetic minerals include minerals containing iron and nickel elements such as magnetite[43, 45]. The MS of diamagnetic minerals typically exhibits negative values, whereas paramagnetic minerals display MS as relatively small positive values. In contrast, ferromagnetic minerals possess MS values that are significantly larger and non-quantitative positive values[43, 46].Usually, terrestrial debris contains more magnetic minerals, so a high magnetic susceptibility may indicate an enhanced input of rivers or wind dust[43, 47-50]. In karst areas, the magnetic susceptibility is also a reliable means of inverting ancient environments[14].

It is generally believed that a warm and humid climate caused by strong summer monsoon may lead to strong chemical weathering and soil formation, which is conducive to the formation of ferromagnetic minerals, and thereby may increase magnetic minerals in sediment and the magnetic susceptibility value. Conversely, a dry and cold climate caused by weak summer monsoon may lead to weak chemical weathering and soil formation, relatively fewer magnetic minerals, and lower magnetic susceptibility values[34, 42, 51]. This is also positively correlated with precipitation and temperature [51-52].

(3) Significance of spore pollen as a climate indicator

The combination of spore pollen fossils in sedimentary strata is closely related to the distribution of vegetation in corresponding geological periods, and different vegetation combinations are strongly influenced by climate[53-54]. Because the high-yielding spore pollen is easily transported and its sporoderm is easily preserved, spore pollen can be used to analyze the properties of plant communities, hence reflecting the background conditions such as climate, paleotopography, and soil, which making the analysis of spore pollen become an important method to reconstruct paleoenvironment and paleoclimate[55-58]. The paleoclimate restoration through analyses of different spore pollen combinations and dominant species has been successfully applied to many different landforms [59-61], including karst landform[62-64].

2.2.2 Testing methods

(1) Method for testing particle sizes

The method for testing particle sizes in this study was based on ZHANG[37] and PAN[65]. The brief steps were as follows: heating 0.5−1.0 g of the sample with 10 ml of 30% hydrogen peroxide to remove organic matter, cooling the sample until no more foaming occurs, adding 10 ml of 10% dilute hydrochloric acid to remove carbonates, and then adjusting the sample to neutrality with supernatant. For the first half hour before measurement, 10 ml of 0.05 mol·L^{-1} sodium hexametaphosphate $(NaPO_3)_6$ solution was added and thoroughly shaken with an ultrasonic shaker so that sediment particles could fully disperse. The measurement was carried out by the Mastersizer 2000 laser particle size analyzer produced by Malvern in the UK, with a measurement range of 0.02−2,000 μm. An average value was taken after three times of measurement. In this study, characteristics of particle size compositions and particle size parameters were used as alternative indicators [28, 66] in the analysis of sedimentary environment. By formula: Φ= −log2D (mm) [34, 67], the particle size was converted into Φ. The granularity parameter was calculated by Folk and Ward formulae:

Median diameter (Md): Md=Φ50

Mean grain size (Mz): Mz=(Φ16+Φ50+Φ84)/3

Sorting coefficient(σ): σ=(Φ84−Φ16)/4+(Φ95−Φ5)/6.6

Kurtosis (Kg): Kg=(Φ95−Φ5)/2.44(Φ75−Φ25)

Skewness (Sk): Sk=(Φ16+Φ84−2Φ50)/2(Φ84−

Φ16)+(Φ95+Φ5−2Φ50)/2(Φ95−Φ5)

Values of Md and Mz reflect the centralized trend of sediment particle size distribution, and lower values reflect larger transport forces and coarser particles. Kg reflects the degree of curve convexity of particle size distribution. The particle size frequency curve of Kg<0.90 shows a gentle trend; 0.90<Kg<1.11 shows normal distribution with a basically symmetrical curve; Kg>1.11 shows a relatively sharp curve. Sk reflects an asymmetric curve of particle size distribution, with negative bias between −1.00 and −0.10, approximate symmetry between −0.10 and 0.10, and positive bias between 0.10 and 1.00. The value of σ indicates the degree of sediment sorting. For example, σ< 0.71 represents good sorting performance; if the value is between 0.71 and 1.00, it represents moderate sorting performance; σ> 1.00 represents low sorting [34].

(2) Method for testing magnetic susceptibility

The method for testing magnetic susceptibility in this study was based on YU et al [68], and ZUO [34]. The magnetic susceptibility meter MS2 of Bartington Instruments in UK was used for measurement. After being dried and crushed, the sample was placed in a 10-milliliter ethylene sample box. Operating frequencies of low frequency (0.47 kHz) and high frequency (4.7 kHz) were respectively selected to measure the low frequency (χlf) and high frequency (χhf) magnetic susceptibilities of the sample [33]. Then the test was repeated three times. Average values of the high and low frequency magnetic susceptibilities were calculated respectively.

Based on the high frequency (HF) and low frequency (LF) susceptibilities, the mass magnetic susceptibility (χ) and frequency magnetic susceptibility (χfd%) of the sample were calculated. The calculation formula (G symbolizing the sample mass) is as follows:

$$\chi = 10 \times \chi lf / G$$

$$\chi fd(\%) = 100 \times (\chi lf - \chi hf)/\chi lf$$

(3) Analysis of spore pollen

The extraction technology of spore pollen is quite mature. Especially in recent years, scholars have improved the original methods for extracting spore pollen on the basis of different regions and lithological characteristics, which has increased the extracting purity [62]. In this study, the Zeiss Scope A1 biofluorescence microscope was used to identify genera and species of spore pollen. They were firstly observed and described systematically so that their basic structures could be determined, based on which the genera and species were identified, starting from major categories. Afterward, the number of each type (or genus) of spore pollen obtained was counted. The proportion of spore pollen was calculated, based on the number of obtained pollen, and then the proportions of different genera and species in different eras were calculated.

3 Results and analyses

3.1 Sedimentary characteristics

(1) Luota section

Based on field observation, Luota section can be divided into 5 layers from the top to the bottom.

0−40 cm: The dark brown modern humus soil layer with loose and porous structure and high organic matter content.

40−150 cm: The brown loose deposit with layer of mud and gravel. This part contains much mud-cemented gravel, with poor roundness and diameters of mostly 4−10 cm.

150−260 cm: Clay Interlayer 1, with gray, black, yellow, and brownish clayey silt and sandy clay. In this study, sampling was started from this layer, below which is the ancient weathering crust, with a total thickness of 350 cm.

260−290 cm: The sand and gravel layer, with brownish-yellow coarse sandstone interbedded with gravel at diameters of 3−8 cm.

290−500 cm: Clay Interlayer 2, with brown-gray clay and yellow-brown clay.

(2) Jiaba section

Based on field observation, Jiaba section can be divided into 3 layers from the top to the bottom:

0−50 cm: The layer of dark gray and black modern

humus soil with loose and porous structure and high organic matter content.

50−350 cm: The silty clay layer with loose structure, mainly composed of siltstone and clay mixed with a small amount of gravel. In this study, sampling was started from this layer. This layer is a typical ancient weathering crust, with a total thickness of 300 cm.

350−650 cm: The stratum of Silurian Xiaoheba Formation (S_1xh), mainly composed of gray-green thin-to-medium-layer siltstone and fine sandstone interbedded with gray shale. Trilobites and graptolites were found in this stratum.

3.2 Sediment composition

(1) Luota section

Analysis of the particle size composition of the weathering crust of Luota section at 150−500 cm (Table 2, Fig.6) revealed that particle sizes of fine sand range from 5 to 50 μm, with an average content of 57.6% in the layer. The content of clay particles ranks second, averaging at 41.9%. The sand content composed of fine sand is the lowest, 0.56%. Overall, the section contains almost no extremely coarse sand or coarse sand.

Table 2 Sedimentary characteristics of Luota section and Jiaba section

Sample	Component/%			Mass MS/ $\times10^{-8}$ $m^3\cdot kg^{-1}$	Sample	Component/%			Mass MS/ $\times10^{-8}$ $m^3\cdot kg^{-1}$	Sample	Component/%					Mass MS/ $\times10^{-8}$ $m^3\cdot kg^{-1}$
	Clay	Silty	Fine sand			Clay	Silty	Fine sand			Clay	Silty	Fine sand	Medium sand	Coarse sand	
LT01	40.16	59.10	0.74	26.25	LT16	42.74	56.83	0.43	17.97	JB01	38.07	53.87	6.39	1.28	0.39	10.31
LT02	41.26	58.24	0.50	16.09	LT17	41.80	57.82	0.38	20.94	JB02	34.84	55.50	8.86	0.67	0.12	11.56
LT03	43.05	56.61	0.35	18.26	LT18	41.72	57.78	0.50	22.50	JB03	41.71	53.92	4.37	0	0	12.66
LT04	39.67	59.77	0.56	24.22	LT19	42.85	56.76	0.39	19.22	JB04	35.91	56.88	7.21	0	0	11.88
LT05	40.17	59.37	0.52	21.88	LT20	41.04	58.41	0.55	24.38	JB05	43.75	52.15	4.11	0	0	11.72
LT06	42.42	57.26	0.32	16.88	LT21	43.01	56.64	0.35	19.38	JB06	41.00	55.76	3.24	0	0	12.03
LT07	42.46	57.14	0.40	19.69	LT22	41.92	57.55	0.53	22.34	JB07	44.22	50.26	5.52	0	0	14.69
LT08	42.86	56.56	0.58	16.72	LT23	39.73	59.65	0.62	10.47	JB08	42.13	52.21	5.66	0	0	15.00
LT09	43.22	56.47	0.32	20.51	LT24	39.73	59.55	0.73	11.72	JB09	37.61	53.22	7.86	0.98	0.33	12.19
LT10	44.55	55.09	0.36	15.16	LT25	42.47	56.97	0.56	11.09	JB10	35.48	51.76	12.07	0.56	0.13	12.19
LT11	42.07	57.60	0.34	18.44	LT26	42.87	56.59	0.55	9.53	JB11	36.27	54.66	8.29	0.62	0.17	14.38
LT12	42.08	57.59	0.33	14.69	LT27	39.46	59.19	1.35	8.59	JB12	36.62	54.69	7.78	0.76	0.16	13.91
LT13	42.91	56.78	0.31	15.47	LT28	41.37	57.35	1.29	10.31	JB13	42.55	51.99	5.46	0	0	14.22
LT14	42.13	56.93	0.94	12.81	LT29	41.66	57.49	0.86	10.63	JB14	36.06	54.97	8.01	0.84	0.12	14.06
LT15	41.97	57.35	0.68	22.81	LT30	42.74	56.79	0.48	11.56	JB15	38.60	58.37	3.03	0	0	14.69

From the vertical curves of different particle sizes in Fig.6, it can be seen that the sand content shows an overall trend of an increase after a decrease from the bottom to the top, which is basically consistent with the variation curve of fine sand content. This result indicates that the sand content in Luota section is mainly controlled by fine sand. However, the curves of silt and clay content are opposite. The curve of clay content shows an overall trend of a decrease after an increase from the bottom to the top. The granularity characteristics show that the same particle size grade varies greatly at different depths and exhibits multiple fluctuations.

(2)Jiaba section

Analysis of particle size composition characteristics of weathering crust in Jiaba section at 50−350 cm shows as below. The weathering crust in Jiaba section are mainly composed of silt with particle sizes ranging from 5 to 50 μm, with an average content of 54%. The average content of clay particles is 39%. The fine sand is the main component of sand particles, with an average content of 6.5%. This section contains very little medium sand and coarse sand, and no extremely coarse sand.

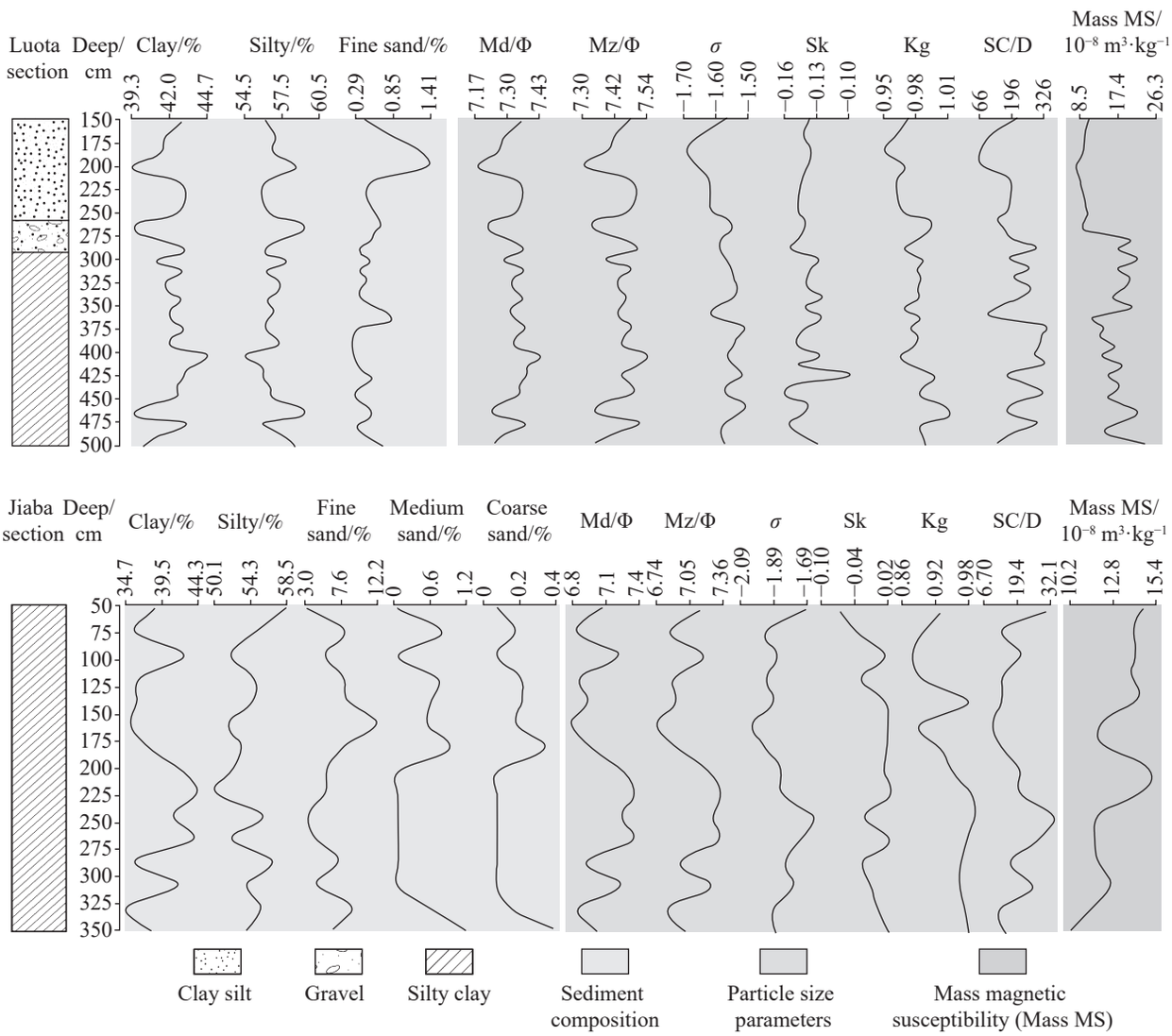

Fig. 6 Vertical variation characteristics of sediment composition, particle size parameter and magnetic susceptibility of weathering crusts in Luota section and Jiaba section

In the composition of sand, the changes of fine sand, medium sand, and coarse sand are relatively consistent, while the changes of silt and clay particles are opposite. The variation amplitude of the same particle size grade is large but the variation is not as frequent as that of Luota section.

3.3 Particle size parameters

(1) Luota section

Particle size parameters of Luota section present the following characteristics: values of Md range from 7.18 to 7.42 Φ, averaging at 7.31Φ; values of Mz range from 7.31 to 7.54 Φ, averaging at 7.44 Φ; values of σ range from −1.68 to −1.51, averaging at −1.57; values of Sk range from −0.16 to −0.1, averaging at −0.14; values of Kg range from 0.95 to 1.01, averaging at 0.98. These characteristics indicate that variation ranges of parameters in Luota section are relatively small. This section is mainly composed of fine particles with excellent sorting performance, and the frequency curve shows an approximately symmetrical distribution with negative bias.

Further analysis of the particle size parameters in Luota section reveals that from the bottom of the section upward, values of Md and Mz show an overall increasing trend in clay interlayer 2, but the fluctuations are more frequent (Fig.6). The lowest value of the section appears in clay interlayer 1. But then the two values gradually increase. Trends of σ and Kg are generally

consistent with each other, with multiple cyclic fluctuations occurring in clay interlayer 2, but the amplitude is relatively small. In the transition part between clay interlayer 1 and the gravel layer, values of σ and Kg decrease significantly and reach the minimum value at about 180−200 cm. After that, the values gradually increase.

Values of SC/D can reflect the dry and wet conditions of the region [41]. The peak range of SC/D values in Luota section corresponds to larger Mz and Md values, with poor sorting performance, reflecting weak winter wind in the region. The increase in seasonal precipitation makes the climate warm and humid, and the enhancement of biochemical processes intensifies sediment weathering and soil formation. The low value range of SC/D reflects strong wind and dry climate. The cyclic curves of particle size parameters at different depths in the section correspond well with the sedimentary cycle of each layer. However, it can also be seen that the parameter curve presents multiple fluctuations in the same layer.

(2) Jiaba section

Analysis of particle size parameters of Jiaba section indicate as follows: values of Md vary from 6.8 to 7.37 Φ, averaging at 7.07 Φ; values of Mz vary from 6.75 to 7.35 Φ, averaging at 7.07 Φ; values of σ vary from 2.07 to −1.7, averaging at −1.9; values of Sk vary from −0.08 to 0.01, averaging at −0.02; values of Kg vary from 0.86 to 0.98, averaging at 0.93. The section is mainly composed of fine particles, with excellent sorting performance and relatively small change of parameters.

3.4 Characteristics of magnetic susceptibility

(1) Luota section

The mass magnetic susceptibility of Luota section ranges from 8.59×10^{-8} to 26.25×10^{-8} $m^3\cdot kg^{-1}$, with an average value of 17.02×10^{-8} $m^3\cdot kg^{-1}$. The maximum frequency of magnetic susceptibility is 9.1%, with an average value of 3.3%. The average mass magnetic susceptibility of the section is less than $20\times10^{-8}m^3\cdot kg^{-1}$. It should be noted that when the mass magnetic susceptibility is less than $20\times10^{-8}m^3\cdot kg^{-1}$, the frequency magnetic susceptibility may reflect measurement errors[69]. Therefore, the magnetic susceptibility discussed in this study only refers to the mass magnetic susceptibility.

From Fig.6, it can be observed that the magnetic susceptibility of Luota section shows an overall decreasing−increasing−decreasing trend in the vertical direction, with an obvious layering variation. There is a significant alternating wave occurring in clay interlayer 2. In addition, magnetic susceptibilities clearly correspond with sediment components and parameters. Magnetic susceptibilities of clay interlayer 2 show different trends in variation with clay and average particle size at different depths. For example, these variables indicate a significant positive correlation at 270−410 cm but a significant negative correlation below 410 cm. In clay interlayer 1, the variation pattern is not obvious. Compared with the variation curve of sand particles, it is found that the value of magnetic susceptibility below 370 cm is generally consistent with that of sand content, but there is a negative correlation at 270−370 cm.

(2) Jiaba section

Values of mass magnetic susceptibilities of Jiaba section range from 10.31×10^{-8} to 15×10^{-8} $m^3\cdot kg^{-1}$, averaging at 13.03×10^{-8} $m^3\cdot kg^{-1}$. The maximum frequency magnetic susceptibility is 7.9%, averaging at 1.82%. The maximum mass magnetic susceptibility is 15×10^{-8} $m^3\cdot kg^{-1}$, less than 20×10^{-8} $m^3\cdot kg^{-1}$.

The overall trend of magnetic susceptibility of Jiaba section shows an increasing−decreasing−increasing characteristic, which is consistent with the trend of Mz values. This trend shows an obvious variation with the curves of clay and sand particles for a certain period. Below 170 cm, the sand particle curve shows a roughly positive correlation with the fluctuation of magnetic susceptibility, while the regular changes are not significant at 50−170 cm. The clay curve shows a negative correlation trend with magnetic susceptibility fluctuations below 200 cm, and a roughly positive correlation trend at 50−200 cm.

3.5 Spore pollen characteristics

After inspection and identification of samples

(Fig.7), it was found that eight samples (LT-1, LT-2, LT-3, LT-7, LT-Y1, LT-Y2, JB-1, and JB-Y1) are rich in spore pollen. However, three samples (LT-4, LT-5, and LT-6) contain relatively little spore pollen, and no spore pollen fossils have been found in three other samples (LT-Y3, JB-2, and JB-3). The detail information is illustrated in Fig.7.

(1) LT-1

Polypodium > 100 granules; *Pinus*: 35 granules

Abies: 4 granules; *Podcarpus*: 2 granules

(2) LT-2

Polypodium: 64 granules; *Pinus*: 8 granules; *Chenopodium*: 1 granule

(3) LT-3

Polypodium: 36 granules; *Pinus*: 2 granules

(4) LT-7

Polypodium: 37 granules; *Pinus*: 2 granules

(5) LT-Y1

Polypodium: 11 granules; *Pinus*: 26 granules; *Abies*: 1 granule

(6) LT-Y2

Polypodium > 100 granules; *Pinus*: 7 granules; *Podcarpus*: 1 granule

(7) JB-1

Polypodium: 7 granules; *Pinus*: 21 granules; *Gramineae*: 1 granule

(8) JB-Y1

Polypodium: 18 granules; *Pinus*: 14 granules; *Carpinipites*: 1 granule; *Gramineae*: 1 granule

(9) LT-4

Polypodium: 1 granule; *Podcarpus*: 1 granule

(10) LT-5

Pinus: 2 granules

(11) LT-6

Pinus: 1 granule

4 Discussion

4.1 Relationship between planation surface and regional karst landform evolution

The current terrain of Hunan is a "horseshoe-shaped" basin surrounded by mountains on three sides—east, west, and south, and gently inclines northward. Wuling, Xuefeng and Mufu Mountains surrounded by the Dongting basin are the strong uplifting areas of the late Himalayan movement. The number of planation surface and valley terrace gradually decreases from west to east, with the corresponding decrease of their altitudes. As a result, the intensity of karstification in the region follows a decreasing trend from low-level to high-level planation surfaces. The high-level planation surface is mainly a recharge area of karst water, characterized by vertical karst forms such as karst depressions, dolines, and ponors. However, runoff and discharge areas are mostly located at the low-level planation surface, mainly characterized by horizontal caves, underground rivers, and rocky desertification areas. [21, 70].

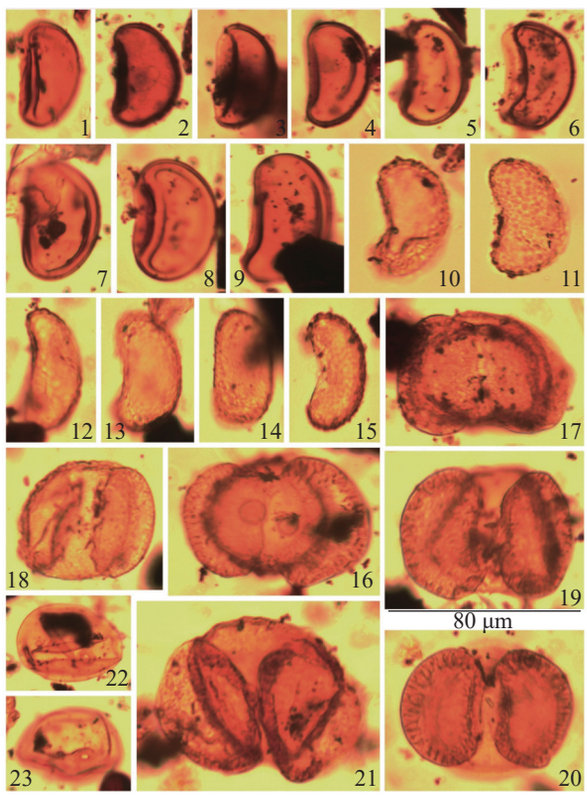

Fig. 7 Sporopollen assemblage chart of Luota section and Jiaba section

1−15. *Polypodium* (sample numbers of 1-9: LT-3; sample numbers of 10−15: LT-Y2); 16. *Podcarpus* (sample number: LT-Y2); 17−21. *Pinus* (sample numbers of 17−20: LT-Y1; sample number of 21: LT-3); 22−23. *Gramineae* (sample number of 22: JB-1; sample number of 23: JB-Y1)

Planation surfaces in Xiangxi are developed in an

imbalanced way in the north and south, with a possible Level-4 planation in the south and a Level-6 in the north [19-21] (Table 1). Generally, a planation surface reflects a stationary stage, at least a relatively long stable period during tectonic uplift. This indicates that Xiangxi, as a geomorphic transformation zone on the edge of the YGP, may be affected by tectonic uplift in a heterogeneous way. From a global perspective, the Paleogene was a favorable period for the development of planation surfaces or the formation of quasi plains. In the late Paleogene to the Neogene, regionally representative planation surfaces during the Luota and Zhaoshi Periods were formed in Xiangxi, with rich karst landforms such as karst hills, dolines, ponors, stone forests, clints, shafts, karst depressions, and valleys. Xiangxi is also characterized by the distribution of recharge and discharge areas, which indicates that the time of karstification from the late Paleogene to the Neogene was relatively long. These characteristics constitute basic conditions for the differences in landforms between Xiangxi and the central-southern Hunan.

Another important condition that causes evolution differences of the regional karst landforms is the paleoclimate. The planation surfaces formed in China during the wet and hot period of the Neogene were developed along the line from Xizang to Yunnan, Hunan and Guizou[71-72]. In the Pliocene, the northern boundary of China's subtropical zone reached around 41 ° N. The influence of wet and hot weather on planation surfaces and karst landforms often crossed geological units and watersheds[73]. In most parts of the karst region in Southwest China, there are weathering crusts overlying different bedrocks. Weathering crusts of the Luota and Zhaoshi Periods in Xiangxi are the products of paleoclimate and paleoenvironment at different times and altitudes, and have an important impact on the series of karst landforms.

4.2 Paleoclimate reflected by weathering crusts on planation surfaces in Xiangxi

Sedimentary records of Luota section show that the weathering crust experienced three significant climate fluctuations: the significantly warming period recorded at 410−500 cm, the decreasing of humidity at 280−410 cm, and the relatively humid period at 150−280 cm. Although the sedimentary curve of the section fluctuates multiple times, its amplitude is relatively small. This indicates that during the sedimentary period, the overall paleoclimate was warm and humid, and river levels were generally high and stable. Contents of clay and silt of the section reached 41.9% and 57.6%, respectively, while the sand content was only 0.56%. The overall high values of Mz, Md, SC/D, and magnetic susceptibility values indicate a relatively humid sedimentary environment. In terms of the sedimentary characteristics of weathering crust, clay interlayers are situated at 290−500 cm and 150−260 cm, and gravel layers at 260−290 cm of Luota section. In clay interlayer 2, the average content of clay particles is 42.1%, and that of sand is 0.47%. The highest value of clay particles (44.55%) and the lowest value of sand particles (0.31%) both occur in this layer. The average values of Mz, Md, and SC/D are 7.45 Φ, 7.33 Φ, and 233.8, respectively. Compared with other sedimentary layers, the climate reflected in clay interlayer 2 was generally the moistest, similar to the climate recorded at 150−260 cm in clay interlayer 1, but the climate reflected in interlayer 1 is more changeable. It is inferred that Luota section reveals the climate experiencing from rewarming period to warm and humid period, and then warm period during sedimentation of the weathering crust on the planation surface in the Luota period.

During the sedimentation of the weathering crust in Jiaba section, the climate also experienced 3 significant fluctuations, namely, the relatively humid period recorded at 230−350 cm, the relatively cool and dry period at 160−230 cm, and the warming period at 50−160 cm. During the relatively humid period at 230−350 cm, contents of clay particles in the section significantly increased, while those of silt and sand particles decreased and reached the lowest value. The overall fluctuation of Mz, Md, SC/D, and magnetic susceptibility values indicate that the climate was relatively humid, the summer monsoon became stronger, and the river level rose dur-

ing this period. During the period recorded at 160−230 cm, the overall contents of clay particles decreased, while the contents of silt and sand particles increased. However, the decrease in clay and the increase in silt and sand were relatively small. Compared to the climate in the previous period, significant decreases of Mz, Md, and SC/D values in this period indicate that the climate during the sedimentation was dry or cool, and the summer monsoon was relatively weak, resulting in a decrease in river levels. During the period recorded at 50−160 cm, there were obvious peak (at 110 cm) and bottom (at 90 cm). But generally, the clay content increased; the sand content significantly decreased; the magnetic susceptibility remained relatively high. The values of Mz, Md, and SC/D showed an increasing trend. These findings may indicate that the climate in this period was relatively humid, with slightly stronger summer monsoon, and river levels remained basically stable. It can be inferred that Jiaba section reveals a climate transition from warm and humid to dry, then to cool and humid, and finally to warming during sedimentation of the weathering crust in the Zhaoshi period.

Although both Luota and Jiaba sections experienced multiple fluctuations during sedimentation, particle sizes and magnetic susceptibilities show that the sedimentary environment of these two sections was generally humid, with relatively small fluctuations of dry period. Moreover, Luota section contains a higher silt content and a significantly lower sand content. The average values of Mz, Md, and magnetic susceptibility are also low, indicating that the sedimentary environment of the weathering crust in Luota section was slightly humid and warm, compared to the same variables of Jiaba section. In addition, a layer of sand gravel was also developed in Luota section, which may represent the rejuvenation of ancient rivers. Therefore, it can be inferred that the sedimentary environment of the weathering crust in Luota section was warm with high humidity, but cool and humid with low humidity in Jiaba section.

4.3 Verification of paleoclimate by spore pollen

Results of spore pollen identification indicate that the types of the spore pollen of the two sections are different. Samples LT-1, LT-2, LT-3, LT-7, LT-Y1 and LT-Y2 from Luota section show moderate abundance and consistent combinations of spore pollen. The main components are *Polypodium* and *Pinus*, and small amounts of *Abies*, *Podcarpus* and *Chenopodium*. Contents of spore pollen in samples LT-4, LT-5 and LT-6 are relatively low, with several of *Polypodium*, *Pinus* and *Podcarpus*. No spore pollen was found in sample LT-Y3. The concentration of spore pollen in samples JB-1 and JB-Y1 of Jiaba section is low, with the main components of *Polypodium* and *Pinus*, and small amounts of *Gramineae* and *Carpinipites*. No spore pollen fossils were found in samples JB-2 and JB-3. This is likely due to the fact that in terms of the location of field sampling, these samples belong to the bedrock with low weathering.

It can be seen that the spore pollen concentration in Luota section is higher, while the concentration in Jiaba section is low. The spore pollen types in both sections are relatively few. Despite some differences in types of spore pollen, there are a large number of *Polypodium* in both of these two sections, suggesting that the climate was warm and hot at that time, which is consistent with the analysis of particle size and magnetic susceptibility. The climate with high temperature and humidity also played an important role in promoting the formation of planation surfaces and the development of other karst landforms.

4.4 Exploration of the erosion age of planation surfaces

The determination of the erosion age of planation surfaces has always been a difficult problem [6-8]. Despite many studies on the planation surface in Xiangxi, the issue on the chronology of planation formation has not been well resolved. According to the study of karst caves and deposits in the Luota area, JIN et al[20] suggested that the development of planation surfaces from the karst tableland at the highest altitude to the valley in this area spanned from the pre-Tertiary to the early-middle Pleistocene. Comparing the lithology and chemical com-

position of the Quaternary deposits in Luota, PENG et al[10] found evidence for early-to-middle Pleistocene sedimentation. On the basis of the residual slope deposits and ice water accumulation of Tiziyan in Luota, CHEN [21] inferred that the highest platform was formed during the Paleogene−Neogene period, while karst landforms, such as stone forests, on the platform were formed between 5,330 to 10 ka.

The spore pollen of weathering crust in Luota section was mainly composed of *Polypodium* and *Pinus* common in the Cenozoic, and small amounts of *Abies*, *Podcarpus* and *Chenopodium*. Spore pollen fossils from the Paleozoic and Mesozoic and fossils clearly indicating the Paleogene were not found. But there were fossils common in the Neogene. Therefore, it is preliminarily speculated that the weathering crust of Luota section may have started sedimentation in the early Neogene, and the Luota planation surface may have been formed in the Miocene.

In Jiaba section, there were small amounts of *Gramineae* and *Carpinipites*, but spore pollen molecules common in the Paleozoic and the Mesozoic and spore pollen fossils clearly indicating the Paleogene were not found. *Gramineae* and *Carpinipites* were mainly from the Neogene−Quaternary. Based on these data, it is inferred that Jiaba Section may have started sedimentation in the early Quaternary, and the Zhaoshi planation surface may have been formed in the Pleistocene.

5 Conclusion

（1）The weathering crust of Luota section is mainly composed of interbedded layers of clay and gravel, with high clay and silt contents and low sand contents. The values of Mz, Md, SC/D, and magnetic susceptibility of the weathering crust are generally high. The weathering crust of Jiaba section is mainly composed of the layer of silt and clay and sandstone, with relatively more fluctuations in values of Mz, Md, SC/D and magnetic susceptibility. Both sections indicate three significant index fluctuations, but the fluctuation of Jiaba section show greater amplitude.

（2）The particle size and magnetic susceptibility of the two sections reflect that the paleoclimate during the formation of weathering crust was generally humid, accompanied by small fluctuations of dry climate. In detail, the climate in the Luota period may have been a warm climate with high humidity, while the climate in the Zhaoshi period may have been a cool climate with low humidity. This finding is consistent with the results of spore pollen analysis. The climate with high temperature and humidity played an important role in promoting the formation of planation surface and the development of karst landforms.

（3）According to the data on spore pollen, it is speculated that the planation surface in the Luota period may have been formed in the Miocene, and the planation surface in the Zhaoshi period may have been formed in the Pleistocene. However, the accurate chronological conclusions cannot be drawn at present. Further research and comparison are needed in the future.

Reference

[1] REN Xuemei, CHEN Zhong, LUO Lixia, ZHOU Xinqin, WANG Jianli. Summary on the study of planation surface[J]. Scientia Geographica Sinica, 2003, 23(1): 107-111.

[2] Coltorti M, Ollier C D. Geomorphic and neotectonic evolution of the Ecuadorian Andes[J]. Geomorphology, 2000, 32(1): 1-19.

[3] 崔之久, 高全洲, 刘耕年, 潘保田, 陈怀录. 夷平面、古岩溶与青藏高原隆升[J]. 中国科学 (D 辑: 地球科学), 1996, 26(4): 378-386,101.

[4] 潘保田, 邬光剑, 王义祥, 刘志刚, 管清玉. 祁连山东段沙沟祁连山东段沙沟河阶地的年代与成因[J]. 科学通报, 2000, 45(24): 2669-2675.

[5] 李吉均. 青藏高原隆起的三个阶段及夷平面[M]. 北京: 中国环境科学出版社, 1995: 1-5.

[6] 崔之久, 李德文, 冯金良, 刘耕年. 夷平面研究的再评述[J]. 科学通报, 2001, 46(21): 1761-1768.

[7] LI Dewen, CUI Zhijiu. Karst planation surface and the Qinghai-Xizang Plateau uplift[J]. Quaternary Sciences, 2004, 24(1): 58-63.

[8] PAN Baotian, GAO Hongshan, LI Jijun. On problems of planation surface: A discussion on the planation surface in Qinghai-Xizang Plateau[J]. Scientia Geographica Sinica, 2002, 22(5): 520-526.

[9] LI Dewen, CUI Zhijiu, LIU Gengnian. A development model of red weathering crust on limestones: An example from Hunan, Guangxi, Guizhou, Yunnan and Tibet[J]. Acta Geographica

Sinica, 2002, 57(3): 293-300.

[10] PENG Hanxing, WU Yingke. Geochemical characteristics of the Quaternary sediments in Luota karst region[J]. Carsologica Sinica, 1985, 4(4): 39-46.

[11] LAO Wenke, LI Zhaolin, LUO Weiquan, LIANG Bin. Main features and classification of epikarst in Luota area[J]. Carsologica Sinica, 2002, 21(1): 32-37.

[12] LI Jijun, FANG Xiaomin, PAN Baotian, ZHAO Zhijun, SONG Yougui. Late Cenozoic intensive uplift of Qinghai-Xizang Plateau and its impacts on environments in surrounding area[J]. Quaternary Sciences, 2001, 21(5): 381-391.

[13] 吴忱, 马永红, 张秀清, 马永红, 赵明轩. 华北山地地形面、地文期与地貌发育史[M]. 石家庄: 科学技术出版社, 1999: 245-252.

[14] FENG Jinliang. Researches in planation surfaces and weathering mantles[D]. Beijing: Peking University, 2002.

[15] WANG Jing'ai, ZUO Wei. Geographic atlas of China[M]. Beijing: Sinomaps Press, 2010.

[16] JIANG Zhongcheng, ZHANG Jing, HUANG Chao, RONG Yuebing, WU Liangjun. Causes of formation and geo-scientific significance of karst gorge group in Xiangxi geopark[J]. Carsologica Sinica, 2019, 38(2): 269-275.

[17] Wu Liangjun, Jiang Haixian, Chen Weihai, Peng Wenhong. Geodiversity, geotourism, geoconservation, and sustainable development in Xiangxi UNESCO Global Geopark: A case study in ethnic minority areas[J]. Geoheritage, 2021, 13(99): 1-18.

[18] WU Liangjun, CHEN Weihai, RONG Yuebing, ZHANG Jing, HUANG Chao, ZHU Haiyan, MENG Qingxin, WU Jiwen, LUO Qukan, BAI Bing, OU Mengmeng. Development characteristics and research value of red carbonate stone forest in the Xiangxi geopark[J]. Carsologica Sinica, 2020, 39(2): 251-258.

[19] CHEN Changming. On the new tectogenesis of northwestern Hunan[J]. Hunan Geology, 1988, 7(2): 64-72.

[20] JIN Liduo, LV Zhongyuan, LIN Yushi, ZHANG Shunzhi. Karst development in Luota area, west Hunan[J]. Carsologica Sinica, 1983, 2(1): 19-30.

[21] CHEN Anze. Karst stone forest landscapes in China[M]. Beijing: Science Press, 2011.

[22] YU Haoran, WU Yingke. An outline of karst geology in Luota region[J]. Carsologica Sinica, 1982, 1(1): 33-39.

[23] YIN Jianjun. Climate change in the past 2000 years revealed by stalagmites from Lianhua cave in northwest Hunan, China[D]. Chongqing: Southwest University, 2013.

[24] ZHANG Huiling, YU Kefu, ZHAO Jianxin, FENG Yuexing, LIN Yushi, ZHOU Wei, LIU Guohui. Variations in deposition rate of sedimentary cycle from a stalagmite in Lianhua cave and its paleoclimatic implications during the mid-late Holocene[J]. Carsologica Sinica, 2017, 36(4): 580-590.

[25] JIANG Duanwu, LI Daming, MEI Jinhua. Karst circle in west-northern Hunan and its neotectonics remote sensing interpretation information[J]. Hunan Geology, 2001, 20(3): 225-229.

[26] 刘钟伟. 湖南省大型矿床成矿大地构造背景: 以湘西北、湘南为例[J]. 国土资源导刊, 2006, 3(3): 46-51.

[27] LIANG Enyun, LIU Wei, LIU Yaorong, HUANG Leqing, LIU Gengyan, PENG Nengli, CAO Jiehua. Research on sedimentary tectonic metallogenic of Hongyanxi area in the northwest Hunan[J]. Geological Survey of China, 2016, 3(4): 29-36.

[28] LI Bin, HU Bowen, LUO Qun, JIN Changhao, WANG Yilin. Tectonic sequence and sedimentary evolution in western Hunan[J]. Marine Origin Petroleum Geology, 2018, 23(1): 1-12.

[29] LAO Wenke, JIANG Zhongcheng, SHI Jian, LIANG Bin. Hydrogeologic structure and feature of the epi-karst in Luota[J]. Carsologica Sinica, 2003, 22(4): 9-17.

[30] DU Yuchao, LIANG Bin, LI Zhaolin. Groundwater dynamics analysis of the saturated karst zone of Luota in Hunan Province[J]. Ground Water, 2006, 28(2): 48-52.

[31] SU Chuntian, PAN Xiaodong, TANG Jiansheng, ZOU Shengzhang, LIANG Xiaoping, LI Zhaolin. Influence of eco-environment on hydrogeochemical of epikarst springs in Luota, west Hunan Province of China[J]. Mountain Research, 2014, 32(2): 205-211.

[32] LAN Funing, WANG Wenjuan, WU Huaying, JIANG Zhongcheng, QIN Xiaoqun, AN Shuqing. Temporal and spatial distributions of CO_2 in soil and their influencing factors under different LUCC: A case study of the Dalongdong underground river drainage area[J]. Carsologica Sinica, 2017, 36(4): 427-432.

[33] XU Shujian, PAN Baotian, ZHANG Hui, LI Qiong. Grain size parameters of loess-palaeosol deposits from graphic and moment methods: A comparative study[J]. Arid Land Geography, 2005, 28(2): 194-198.

[34] ZUO Hailing. The sedimentary environmental evolution since the Holocene in the Maqu plateau recorded by Langqu section[D]. Lanzhou: Northwest Normal University, 2016.

[35] 丁仲礼, 任剑璋, 刘东生, 孙继敏, 周晓权. 晚更新世季风—沙漠系统千年尺度的不规则变化及其机制问题[J]. 中国科学 (D 辑: 地球科学), 1996, 1(5): 385-391.

[36] Ding Zhongli, Sun Jimin, Liu Dongsheng. A sedimentological proxy indicator linking changes in loess and deserts in the Quaternary[J]. Science in China, 1999, 42(2): 146-152.

[37] ZHANG Wenli. The desertification evolution reflected by grain-size and magnatic susceptibility in Maqu plateau since Middle-late Holocene[D]. Lanzhou: Northwest Normal University, 2015.

[38] 鹿化煜, 安芷生. 洛川黄土粒度组成的古气候意义[J]. 科学通报, 1997, 42(1): 66-69.

[39] 陈骏, 季峻峰, 仇纲, 朱洪兵, 鹿化煜. 陕西洛川黄土化学风化程度的地球化学研究[J]. 中国科学 (D 辑: 地球科学), 1997, 2(6): 531-536.

[40] LIU Bing, JIN Heling, SUN Zhong, SU Zhizhu, ZHANG Caixia. Geochemical characteristics of Aeolian deposits in Gonghe basin, northeastern Qinghai-Tibetan Plateau and the indicating climatic changes[J]. Advances in Earth Science, 2012, 27(7): 788-799.

[41] YU Xuefei, LI Baosheng, JIN Heling, LV Yuxiao. Grain-size cycles during the last interglacial period in the Salawusu river

valley responding to the past global change[J]. Journal of South China Normal University (Natural Science Edition), 2004, 31(1): 129-135.

[42] HU Mengjun, LI Sen, GAO Shangyu, ZHANG Dengshan. Evolution process of land desertification around Qinghai lake since 32 ka BP reflected by sediment grain-size features[J]. Journal of Desert Research, 2012, 32(5): 1240-1247.

[43] LI Shan, WU Huaichun, FANG Qiang, XU Junjie, SHI Meinan. Cyclostratigraphy of the Devonian/Carboniferous boundary sections in South China[J]. Earth Science Frontiers, 2022, 29(3): 329-339.

[44] WANG Jian, LIU Zechun, JIANG Wenying. A relationship between susceptibility and grain-size and minerals, and their paleo-environmental implications[J]. Acta Geographica Sinica, 1996, 51(2): 155-163.

[45] Ellwood B B, Crick R E, Hassani A E, Benoist S L, Young R H. Magnetosusceptibility event and cyclostratigraphy method applied to marine rocks: Detrital input versus carbonate productivity[J]. Geology, 2000, 28(12): 1135-1138.

[46] XUE Xiangxu, ZHAO Jingbo. Characteristics and significance of the micromorphology of Neogene red clay of Xunyi, Shaanxi Province[J]. Acta Sedimentologica Sinica, 2003, 21(3): 448-451,481.

[47] Stage M. Magnetic susceptibility as carrier of a climatic signal in chalk[J]. Earthand Planetary Science Letters, 2001, 188(1-2): 17-27.

[48] Rey D, Rubio B, Mohamed K, Vilas F, Alonso B, Ercilla G, Rivas T. Detrital and early diagenetic processes in Late Pleistocene and Holocene sediments from the SW Galicia Bank inferred from high-resolution enviromagnetic and geochemical records[J]. Marine Geology, 2008, 249(1-2): 64-92.

[49] Hladil J, Cejchan P, Babek O, Koptikova L, Navratil T, Kubinova P. Dust-A geology-orientated attempt to reappraise the natural components, amounts, inputs to sediment, and importance for correlation purposes[J]. Geologica Belgica, 2013, 13(4): 367-384.

[50] Maher B A. The magnetic properties of Quaternary Aeolian dusts and sediments, and their palaeoclimatic significance[J]. Aeolian Research, 2011, 3(2): 87-144.

[51] Han J M, Jiang W Y, Liu D S, Lyu H Y, Guo Z T, Wu N Q. Carbonate isotopic records of paleoclimate changes in Chinese loess[J]. Science in China (Earth Sciences), 1996, 39(5): 460-467.

[52] 胡守云, 邓成龙, Appel E, Verosub K. 湖泊沉积物磁学性质的环境意义[J]. 科学通报, 2001, 46(17): 1491-1494.

[53] 施雅风. 中国全新世大暖期气候与环境[M]. 北京: 海洋出版社, 1992: 1-212.

[54] GONG Shengli, BI Ligang. Palynological sedimentation and its relationship with Neogene sedimentary environment in PL19-3 area[J]. China Offshore Oil and Gas (Geology), 2001, 15(6): 388-392.

[55] FENG Xiaohua, YAN Shun, NI Jian. Pollen-based reconstruction of vegetation in Xinjiang during the Holocene[J]. Quaternary Sciences, 2012, 32(2): 304-317.

[56] SHAO Zhaogang, MENG Xiangang, ZHU Dagang, YANG Chaobin, LEI Weizhi, WANG Jin, HAN Jian'en, YU Jia, MENG Qingwei, QIAN Cheng, HE Chengguang. Sporopollen record in the Kongma basin of the Naqu, Tibet, and their environmental significance[J]. Earth Science: Journal of China University of Geosciences, 2013, 38(Suppl.1): 1-9.

[57] WANG Weiming. Progress and prospect of studies on palynology in China[J]. Acta Palaeontologica Sinica, 2009, 48(3): 338-346.

[58] 黄文. 中国孢粉学研究进展[J]. 科技视界, 2014(1): 143-144.

[59] LV Kexin, SHI Guangyao, ZHANG Huan, ZHANG Jinlong, LI Qingzhe, ZHANG Pengcheng. Quaternary palynological records and climatic signifiance of S9 borehole in Sanhe City of Hebei plain[J]. Geological Survey of China, 2022, 9(1): 64-72.

[60] CHEN Ping, WANG Ren, QIN Jungan, YANG Rui, LI Jun, RUAN Zhimei. Oligocene–Miocene palynostratigraphy and paleoclimate of Well WN-A from deep water area, southeast Hainan basin[J]. Journal of Jilin University: Earth Science Edition, 2022, 52(2): 390-402.

[61] YU Junjie, PENG Bo, LAN You, WU Bin, WANG Jilong, DING Dalin, LAO Jinxiu, LI Shuaili, DAI Lu. Palynological record revealed anthropogenic deforestation, sea level and climate changes since marine isotope stage 5a in the northeastern coast of Fujian Province[J]. Earth Science, 2021, 46(1): 281-292.

[62] ZHAO Zengyou. A study on human activities changes and its impact on envirionment during the past 1600 years in Guangxi and Chongqing, based on pollen-spore and charcoal data[D]. Chongqing: Southwest University, 2013.

[63] ZHOU Jianchao, QIN Jungan, ZHANG Qiang, ZHANG Chunlai, JIANG Shiqing. Vegetation, climate and depositional environment changes since the middle Holocene in the karst area of Guilin, Guangxi[J]. Chinese Science Bulletin, 2015, 60(13): 1197-1206.

[64] WANG Qirong, JIANG Yongjun, HAO Xiudong, QIAO Yina, ZHANG Caiyun, MA Lina, MAO Yang, LV Tongru, QIU Ju. A 700-year record of vegetation and rocky desertification evolution based on palynological data of the karst valley area, Chongqing City, China[J]. Acta Ecologica Sinica, 2021, 41(9): 3634-3644.

[65] PAN Ninghui. The climate and environmental evolution and aeolian activity since the Holocene in the Gonghe basin recorded by Masi section[D]. Lanzhou: Northwest Normal University, 2017.

[66] WANG Yong, CAI Yunfeng, LI Guo, LIU Mengjiao, ZHANG Yaohua. On soil magnetic susceptibility of karst district of Chongqing under different rocky desertification[J]. Journal of Southwest China Normal University (Natural Science Edition), 2016, 41(11): 49-55.

[67] 吴正. 风沙地貌学[M]. 北京: 科学出版社, 1987.

[68] 于寒, 黄书捷. 湘江下游漫滩沉积物粒度和磁化率特征研究[C]//第 31 届中国气象学会年会 S11 第三届城市气象论坛—城市与环境气象, 2014.

[69] 宋春晖, 高东林, 方小敏, 崔之久, 李吉均, 杨胜利, 金洪波, Douglas Burbank, Joseph L Kirschvink. 青藏高原昆仑山垭口盆地晚新生代高精度磁性地层及其意义[J]. 科学通报, 2005, 50(19): 2145-2154.

[70] GONG Shuhua, ZHU Lifen. Influence of geological and geomorphologic features on karst rocky desertification in northwestern Hunan Province: A case study of Zhangjiajie City[J]. Carsologica Sinica, 2021, 40(3): 504-512.

[71] XIE Shiyou, YUAN Daoxian, WANG Jianli, KUANG Mingsheng. Features of the planation surface in the surrounding area of the Three Gorges of Yangtze[J]. Carsologica Sinica, 2006, 25(1): 40-45.

[72] WU Jiwen, WU Liangjun, LV Yong, WANG Pujun, ZHOU Jiaming, LIN Yu, PAN Ming, LIAO Jiafei, MENG Qingxin. Transpressional structure and its control on development of Yinchangping dolomite karst system in Lushui City, Yunnan[J]. Carsologica Sinica, 2021, 40(5): 793-804.

[73] LUO Shuwen, HE Wei, YANG Tao, DENG Yadong, LV Yong, WU Kehua, MENG Qingxin. Geological significance of the development characteristics of karst geomorphology and its formation mechanism in Hunan-Guangxi corridor[J]. Carsologica Sinica, 2021, 40(5): 750-759.

《Monitoring and Early Warning Technologies on Karst Lands》一书将出版发行

近日，中国地质调查局岩溶地质研究所蒋小珍研究员团队编著的《Monitoring and Early Warning Technologies on Karst Lands: Surface Collapse and Groundwater Contamination》由德国 Springer 公司作为“Advances in Karst Science”系列丛书将正式出版发行。

该书由袁道先院士作序，内容包括岩溶地形对塌陷和地下水污染的敏感性分析、岩溶塌陷监测预警方法研究、地球物理技术在岩溶塌陷识别和监测中的应用、基于光纤传感技术的岩溶塌陷监测预警方法、岩溶水动力监测在岩溶塌陷风险评估中的应用、高速公路暴雨径流对岩溶水污染的探测与减轻途径、废物处理设施污染物排放渗流通道的早期检测识别等七大部分，该书极大丰富了岩溶科学研究内容，为防灾减灾提供了科技支撑，与世界分享了我国岩溶灾害监测预警研究成果和经验。

（供稿: 戴建玲）